Protein Engineering, Design & Selection, 2017, vol. 30 no. 1, pp. 47–55
doi: 10.1093/protein/gzw062
Advance Access Publication Date: 24 November 2016
Original Article

OXFORD

Original Article

Chaetomium thermophilum formate dehydrogenase has high activity in the reduction of hydrogen carbonate (HCO_3^-) to formate

Aşkın Sevinç Aslan[1], Jarkko Valjakka[2], Jouni Ruupunen[2], Deniz Yildirim[3], Nicholas J. Turner[4], Ossi Turunen[5,*], and Barış Binay[6,*]

[1]Department of Chemistry, Gebze Technical University, Gebze 41400, Kocaeli, Turkey, [2]BioMediTech, University of Tampere, Finland, [3]Vocational School of Ceyhan, University of Cukurova, Adana, Turkey, [4]School of Chemistry, University of Manchester, Manchester Institute of Biotechnology, 131 Princess Street, Manchester M1 7DN, UK, [5]Department of Biotechnology and Chemical Technology, School of Chemical Technology, Aalto University, FI-00076 Aalto, Finland, and [6]Department of Bioengineering, Gebze Technical University, Gebze 41400, Kocaeli, Turkey

Edited by: Alan Berry

[*]To whom correspondence should be addressed. E-mail: Ossi.Turunen@aalto.fi (O.T.); binaybaris@gmail.com (B.B.)

Received 2 July 2016; Revised 21 October 2016; Editorial Decision 21 October 2016; Accepted 7 November 2016

Abstract

While formate dehydrogenases (FDHs) have been used for cofactor recycling in chemoenzymatic synthesis, the ability of FDH to reduce CO_2 could also be utilized in the conversion of CO_2 to useful products via formate ($HCOO^-$). In this study, we investigated the reduction of CO_2 in the form of hydrogen carbonate (HCO_3^-) to formate by FDHs from C*andida methylica* (CmFDH) and *Chaetomium thermophilum* (CtFDH) in a NADH-dependent reaction. The catalytic performance with HCO_3^- as a substrate was evaluated by measuring the kinetic rates and conducting productivity assays. CtFDH showed a higher efficiency in converting HCO_3^- to formate than CmFDH, whereas CmFDH was better in the oxidation of formate. The pH optimum of the reduction was at pH 7–8. However, the high concentrations of HCO_3^- reduced the reaction rate. CtFDH was modeled in the presence of HCO_3^- showing that it fits to the active site. The active site setting for hydride transfer in CO_2 reduction was modeled. The hydride donated by NADH would form a favorable contact to the carbon atom of HCO_3^-, resulting in a surplus of electrons within the molecule. This would cause the complex formed by hydrogen carbonate and the hydride to break into formate and hydroxide ions.

Key words: biotransformation of CO_2, catalytic mechanism, kinetic parameters with hydrogen carbonate, molecular modeling, NAD^+-dependent formate dehydrogenase

Introduction

Running of industrial economy mostly depends on the creation of sustainable energy generation. Therefore, to defeat the energy crisis, the energy industry is inventing new ways to extract energy from carbon-free renewable power such as geothermal, wind, solar power and biofuels. However, often these methods have inherent limitations since they require high temperatures, pressures or high energy in various forms, and also they result in low yields. In addition, generation of these energy forms does not contribute to the reduction of

© The Author 2016. Published by Oxford University Press. All rights reserved. For permissions, please e-mail: journals.permissions@oup.com

Downloaded from https://academic.oup.com/peds/article-abstract/30/1/47/2585061 by Cukurova University Library (CU) user on 09 June 2020

CO_2 emissions. Therefore, methods based on power generation with carbon dioxide capture and sequestration are potentially very promising global strategies (Baxter *et al.*, 2009).

The biotransformation of CO_2 into various energy sources becomes increasingly important due to coupled reduction of CO_2. Photosynthetic organisms like plants and algae can use solar energy, CO_2 and other nutrients and then offer ready energy sources to produce renewable biofuels even on industrial scale. However, many limitations were reported for the upstream and downstream processes, e.g. in biodiesel production from microalgae (Mallick *et al.*, 2016). Plants use photosynthesis to make various carbohydrates from CO_2 and H_2O, but artificial photosynthesis is not currently efficient enough to produce energy carriers and needs further development (Bonke *et al.*, 2015).

Therefore, despite well-known advantages of biocatalysts, the possible biocatalytic conversions of CO_2 directly into fuels and chemicals are very challenging. However, only few biocatalysts are able to capture CO_2, but in principle, they could be engineered for more efficient conversion of CO_2 to hydrocarbons (Shi *et al.*, 2015). An attractive option has been studied in recent years: conversion of greenhouse CO_2 directly into biofuel or chemicals by photosynthetic bacteria. Fast growing cyanobacteria are studied to transform CO_2 to hydrocarbons. In recent years, there has been developed several strategies to transform CO_2 into useful products by various research groups, including the utilization of microbial photosynthesis (Atsumi *et al.*, 2009). One of the latest designed methods is based on using metal catalysts in different buffers: this strategy was reported by Moret *et al.*, (2014). The obtained formic acid was 0.2 M without the need of any bases, amines or buffers. However, required ruthenium catalyst for hydrogenating CO_2 to formic acid is still too expensive. Another strategy is to design bioelectrochemical system using the enzyme as catalyst at cathode in its free form to reduce CO_2 into formic acid (Srikanth *et al.*, 2014). Early saturation of reaction mixture and stability of the enzyme activity are defined as the main problems in the designed reactor.

Several enzymes in various metabolic pathways are able to capture CO_2, and they could be engineered for more efficient conversion of CO_2 to hydrocarbons. One enzymatic strategy is to utilize formate dehydrogenases for production of formate by reduction of CO_2 (Kuwabata *et al.*, 1994; Lu *et al.*, 2006; Hartmann and Leimkühler, 2013; Bassegoda *et al.*, 2014). FDHs catalyze the conversion between formate and CO_2. The active site of FDHs contains complex cofactor molecules. In reducing CO_2 to formate, low activity and low stability has been a problem of FDHs.

It has been shown earlier that NAD-dependent FDHs show a stronger preference to reduce CO_2 than metal-dependent enzymes (Alissandratos *et al.*, 2013; Choe *et al.*, 2014). $NAD(P)^+$-dependent FDH catalyzes conversion of formate anion to CO_2 coupled with the conversion of $NAD(P)^+$ to NAD(P)H, a reaction that can go also to reverse direction from CO_2 to formate (Alissandratos *et al.*, 2013; Kim *et al.*, 2014). For a long time, FDHs have been regarded as only promising biocatalysts for regenerating NADH as cofactor utilized in the biocatalytic synthesis of chiral pharmaceutical intermediates and chemical compounds (Tishkov and Popov, 2004). Only a few FDHs have been analyzed for catalysing the formate production. While NAD-independent FDHs are too oxygen-labile for practical use, promising NAD-dependent FDHs with high CO_2-reducing capacity have been recently found from *Thiobacillus* (Choe *et al.*, 2014; Kim *et al.*, 2014). FDHs of acetogens, including *Clostridia*, take part in a carbon fixation metabolic pathway producing acetate; the first step involves reduction of CO_2 to formate. A new FDH gene from *Clostridium carboxidivorans* was reported as an alternative FDH to reduce CO_2 (Alissandratos *et al.*, 2013). However, no profound characterization study has been reported for this enzyme.

Our previous research interest *Candida methylica* FDH (CmFDH) and *Chaetomium thermophilum* FDH (CtFDH) have not investigated for their CO_2 reduction potential (Ozgun *et al.*, 2015; Binay *et al.*, 2016). In this study, in order to measure this potential, interconversion of formate anion to carbon dioxide coupled with the conversion of $NAD(P)^+$ to NAD(P)H reactions by FDHs were kinetically characterized with hydrogen carbonate as substrate instead of CO_2. The most efficient FDH (CtFDH) in the reduction of hydrogen carbonate to formate was modeled to understand better the reduction mechanism for designing novel FDHs.

Materials and methods

Materials

All chemicals were purchased from Sigma-Aldrich unless noted otherwise. Page Ruler Prestained Protein Ladder (#26616) was purchased from Life Technologies. Ni-NTA His-Trap column was purchased from GE.

Production of purified recombinant FDHs

The previously constructed gene for *Chaetomium thermophilum* FDH enzyme in His-Tagged pQE-2 plasmid was used in the experiments (Ozgun *et al.*, 2015). The gene for *Candida methylica* FDH enzyme was kindly provided by Dr Ayhan Çelik. *fdh*s were expressed in *E. coli* BL21 (DE3) cells (New England Biolab). After cultivation, the cells were disrupted, and the proteins were concentrated and purified with ultracentrifuge tubes having 30 kDa cellulose membrane pore size (MM Amicon Ultracel −30 K). Both CmFDH and CtFDH having N-terminal hexa-histidine tag were then purified with TAGZyme purification system (QIAGEN). The concentrations of the purified FDHs were determined by BCA Protein Assay Kit (Thermo Fischer Scientific).

Activity assays of for formate oxidation and $NaHCO_3$ reduction

The pH-dependent activity of CmFDH and CtFDH was determined by monitoring the absorbance changes at 340 nm due to change in extinction of the cofactor catalyzed redox reaction by the FDHs. In proper pHs at 25°C, the selected 20 mM buffers containing 10 mM sodium formate/sodium hydrogen carbonate and 1.0 mM NAD^+/NADH was used for determining specific activity. The selected 20 mM buffers were acetate for pH 4–6, $KHPO_4$ for pH 6–8, Tris–HCl for pH 7–9 and glycine for pH 9.5–11.5. The purified protein was used in the activity assays (Fig. 1). The specific activity of both FDHs was measured in the presence of 100 µL of NAD^+ solution (10 mM) for 200 mM sodium formate or 50 mM sodium hydrogen carbonate, in 20 mM acetate pH 5 buffer or 20 mM phosphate pH 8 buffer, respectively, at 25°C.

Enzyme kinetic assays

The kinetic assays were done for purified CmFDH and CtFDH in their optimal pH and buffer: 20 mM acetate pH 5 for CtFDH and 20 mM phosphate pH 8 for CmFDH with formate as substrate and 20 mM phosphate pH 7.5 for CmFDH and 20 mM phosphate pH 8 for CtFDH. with hydrogen carbonate as substrate. All reactions

Downloaded from https://academic.oup.com/peds/article-abstract/30/1/47/2585061 by Cukurova University Library (CU) user on 09 June 2020

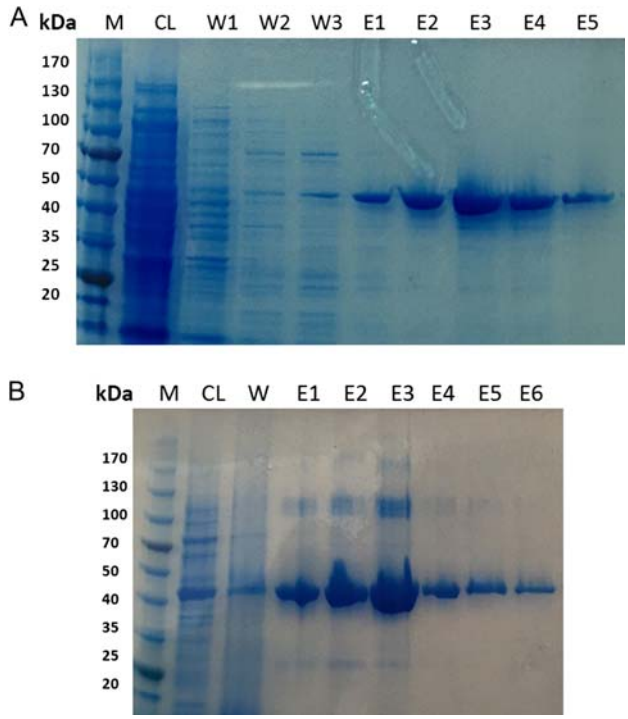


Fig. 1 SDS-PAGE analysis of purified FDHs. (**A**) CmFDH; (**B**) CtFDH. Lanes: M, marker; CL, cell lysate; W, column washing solution; E, eluted fractions

were at 25°C. The forward and reverse reactions were determined by monitoring the changing absorbance at 340 nm due to increasing or decreasing amount of NADH. The reaction mixtures contained 1.0 mM NAD^+ or 0.1 mM NADH, when kinetic parameters were measured for formate and hydrogen carbonate, respectively. The concentration range for measuring kinetic parameters was 0–40 mM for formate and 0–4 mM for hydrogen carbonate. The 10 mM sodium formate was used in determining the kinetic parameters for NAD^+ and NADH. Thus, the Michaelis–Menten kinetic constants were determined from triplicate measurements of the initial velocities by varying the concentrations of one substrate at fixed and saturating concentration of the second compound. The k_{cat} and K_m values were determined by hyperbolic regression analysis.

Biotransformation

To determine the effect hydrogen carbonate concentration on the productivity of CmFDH and CtFDH, the reaction was performed for the different initial hydrogen carbonate concentrations ranging from 2.5 to 500 mM. Briefly, 2.55 ml of phosphate (20 mM, pH 8.0) or acetate buffer (20 mM, pH 5.0), 50 µl enzyme solution (7.5 µg/ml CmFDH or CtFDH, respectively) and 100 µL of NAD^+ solution (10 mM) were mixed in a test tube at 25°C. The reaction was started by the addition of 500 µl bicarbonate solution with the desired concentration. After 15 min reaction time, 20 µl aliquot was withdrawn from the reaction mixture and diluted with 80 µl of H_2SO_4 (0.25 M in water). The formed formic acid amount was detected by using high-performance liquid chromatography (HPLC, Shimadzu Prominence) equipped with a diode array detector (Shimadzu SPD-M20A) at 210 nm (see Fig. S3 for standard graph). The mobile phase was 20 mM H_2SO_4 with a flow rate of 1.0 ml/min. The used column was an anion exclusion column (Alltech Anion Exclusion IC Col-MF, 100×7.5 mm). An oven (Shimadzu CTO-10AS) was used to keep the column temperature at 30 °C during the analysis. To determine the effect of CtFDH amount on the formate production, the reaction was performed for the different enzyme amounts (3.75–30 µg/ml) at 25°C at the hydrogen carbonate concentration of 5 mM and reaction time of 15 min. To determine the effect of reaction time on the activity of CtFDH, the reaction was performed for different time courses ranging from 15 to 120 min at the hydrogen carbonate concentration of 5 mM and enzyme amount of 30 µg/ml.

Modeling the active site of CtFDH

The model of CtFDH was generated with Swiss-Model (http://swiss-model.expasy.org/) using the crystal structure of Pseudomonas sp. 101 FDH (PDB structure 2NAD, Lamzin *et al.*, 1994) as modeling template. For modeling hydrogen carbonate, it was transferred manually into the active site of 2NAD. The hydrogen carbonate was placed at 2.6 Å distance to carbon 4 (C4) of NADH. The orientation was arranged so that the p orbitals of hydrogen carbonate point perpendicularly towards the hydride (H^-) at C4 position. This allows the hydride ion (H^-) to move away from NADH cofactor (Schirwitz *et al.*, 2007). The hydride consists of two electrons in the field of a proton and a rather diffuse electron cloud. The figure was created with PyMOL (http://pymol.org/), and the reaction mechanism was drawn by ChemDraw Professional (Perkin Elmer).

Results and discussion

Production of purified recombinant FDHs and biochemical characterization

Purified FDH enzymes (Fig. 1) were used to study their catalytic properties with formate and $NaHCO_3$ as substrate. Hydrogen carbonate was used as CO_2 source due to its stability and convenience in the experimental work (Choe *et al.*, 2014). With hydrogen carbonate, CmFDH and CtFDH showed the pH optimum at pH 7–8, also depending on the buffer (Fig. 2 A). Both FDHs start to lose their activity while pH decreases. In the lowest measured pH (pH 5), CtFDH and CmFDH showed about 50% and 32% activity, respectively. While pH increases from neutral, both FDHs showed high activity up to pH 9.5. In the highest measured basic pH (pH 11.5), CmFDH and CtFDH showed only 14% and 35% activity, respectively. CtFDH showed slightly wider pH activity profile than CmFDH with hydrogen carbonate. Under acidic conditions, NADH is gradually degraded, which also leads to decreased formation of formate (Wu *et al.*, 1986).

When formate was the substrate, both enzymes showed quite high activity in a wide pH region (5.0–11.5) (Fig. 2B), and the pH activity profiles with formate were slightly wider than with hydrogen carbonate. CtFDH showed the highest activity at pH 5 and CmFDH at pH 8 with formate (Fig. 2B).

Enzyme specific activity and kinetic assays

The specific activities measured in fixed substrate concentration (200 mM for formic acid and 50 mM for sodium hydrogen carbonate) showed that CtFDH appears to transform hydrogen carbonate to formate by the highest rate among the known FDH enzymes (Table I). However, in the oxidation of formate, CtFDH belongs to the weakest group of enzymes. When comparing CtFDH and CmFDH, CtFDH was stronger than CmFDH in the reduction of hydrogen carbonate, and CmFDH was stronger in the oxidation of

Downloaded from https://academic.oup.com/peds/article-abstract/30/1/47/2585061 by Cukurova University Library (CU) user on 09 June 2020

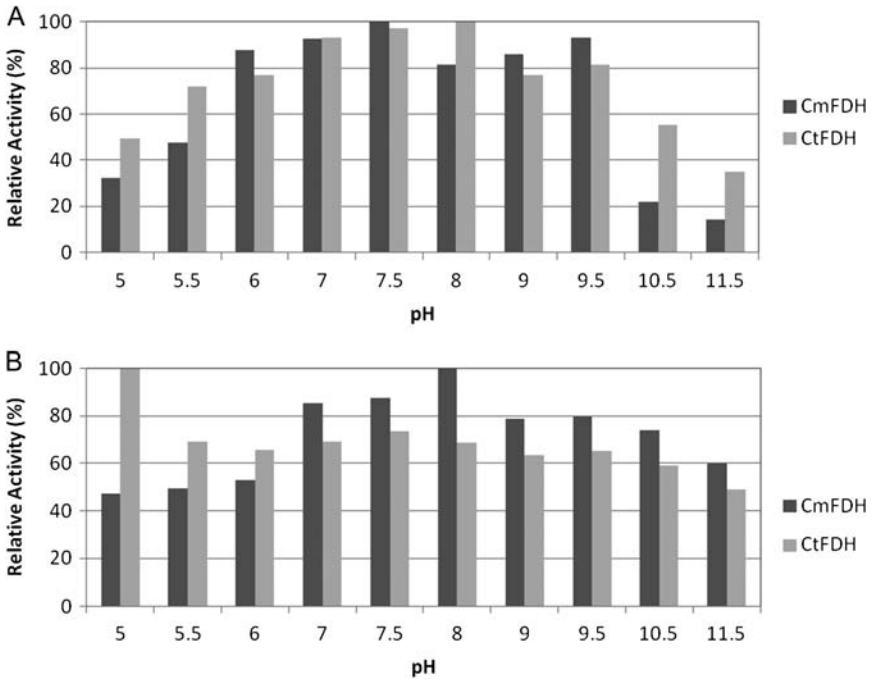


Fig. 2 Effect of pH on activity with hydrogen carbonate and formate. Substrate: (**A**) bicarbonate; (**B**) formate. Used buffers were pH 5, 5.5, 6—Acetate buffer; pH 6, 7, 7.5, 8—Phosphate buffer; pH 7, 7.5, 8, 9—Tris-HCl buffer; 9.5, 10.5—Glycine buffer; the order of the columns is according to these buffers. CtFDH, black columns; CmFDH, gray columns.

Table I. Specific activities of the FDHs on formate oxidation and CO_2 reduction

FDHs[a]	Optimum pH[b]		Activity at optimum pH[a]		References
	Formate oxidation	CO_2 reduction[c]	Formate oxidation [U/mg enzyme]	CO_2 reduction[b] [mU/mg enzyme]	
AaFDH	6.0	6.0	21.6 ± 0.23	4.5 ± 0.22	Choe *et al.*, (2014)
CbFDH	7.0	5.5	6.1 ± 0.02	1.6 ± 0.08	Choe *et al.*, (2014)
CsFDH	6.5	6.0	1.3 ± 0.10	0.8 ± 0.03	Choe *et al.*, (2014)
MsFDH	5.5	5.5	14.3 ± 0.10	2.8 ± 0.12	Choe *et al.*, (2014)
PsFDH	5.5	5.5	12.2 ± 0.40	6.5 ± 0.06	Choe *et al.*, (2014)
TsFDH	6.5	5.5	10.9 ± 0.34	12.2 ± 0.13	Choe *et al.*, (2014)
CtFDH	5.0	5.0	3.1 ± 0.10	34.6 ± 0.07	This study
CmFDH	8.0	8.0	13.2 ± 0.12	4.7 ± 0.03	This study

[a]*Ancylobacter aquaticus* (Aa), *Candida boidinii* (Cb), *Ceriporiopsis subvermispora* (Cs), *Moraxella sp*. C-1 (Ms), *Paracoccus sp*. 12-A (Ps), *Thiobacillus sp*. KNK 65MA (Ts).

[b]These values were determined from the results in Fig. 2.

[c]The activity of CO_2 reduction was determined using sodium bicarbonate as described in Materials and Methods.

formate (Table I). CtFDH could be a promising enzyme for further development of CO_2 reduction.

The purified enzymes were used for kinetic assays with both formate and hydrogen carbonate. The calculated kinetic parameters of CtFDH and CmFDH for formate and hydrogen carbonate are shown in Table II and for NAD^+ and NADH in Table S1. The corresponding Michaelis–Menten reaction graphs are shown in Fig. S1. When comparing CtFDH and CmFDH, the experimental results showed that CtFDH has lower K_m and higher k_{cat} both with formate and hydrogen carbonate than CmFDH. The resulting catalytic performance (k_{cat}/K_m) of CtFDH was ~3-fold higher with formate and ~6-fold higher with hydrogen carbonate than the performance of CmFDH. Therefore, the k_{cat}/K_m values do not reflect the higher specific activity of CmFDH in high substrate concentration (200 mM formate), probably because the testing substrate concentration was much above the K_m concentration (7 mM for CmFDH and 3.3 mM for CtFDH).

Among FDHs, especially *Pseudomonas* sp. (strain 101) (PseFDH), *Candida boidinii* (CbFDH), *Thiobacillus* sp. (strain KNK65MA) (TsFDH), *Candida methylica* (CmFDH) and *Chaetomium thermophilum* (CtFDH) could be attractive for not only to produce NAD(P)H, but also for reduction of CO_2 to formic acid. When comparing kinetic constants of CtFDH and CmFDH with other studies, CtFDH showed high k_{cat} and catalytic efficiency (k_{cat}/K_m) for formate (Table II). For hydrogen carbonate, the k_{cat} of TsFDH was the highest but the specific activity was the highest in CtFD (Tables I and II). Furthermore, to evaluate the industrial potential, the formate productivity in high concentration of hydrogen carbonate or CO_2 should be tested.

The examination of kinetic parameters reveals a basic feature that K_m for formate was about 10-fold higher than for hydrogen

Downloaded from https://academic.oup.com/peds/article-abstract/30/1/47/2585061 by Cukurova University Library (CU) user on 09 June 2020

carbonate in CtFDH and CmFDH. Still the k_{cat} for oxidation of formate was much faster than for reduction of hydrogen carbonate (Table II). This might indicate that although hydrogen carbonate apparently binds much better to the enzyme, the hydride transfer from formate to NAD^+ appears to be much faster than the hydride transfer from NADH to HCO_3^-. However, Choe *et al.* (2014) calculated the binding affinity constant K_B under non-steady state condition, which did not in CbFDH and TsFDH differ in any greater extent between formate and hydrogen carbonate (Table II). Further research is needed for understanding better the hydride transfer in the reduction of HCO_3^- and CO_2.

Biotransformation

The capability of CtFDH and CmFDH to produce formate was measured in higher substrate (hydrogen carbonate) concentrations by following the accumulation of formic acid by HPLC. The effect of initial substrate concentration on the production of formic acid is shown in Fig. 3. The results are in line with the kinetic data (Tables I and II) that CtFDH has stronger ability to transform hydrogen carbonate to formate than CmFDH. However, in CtFDH at the hydrogen carbonate concentration higher than 5 mM, the formed formic acid amount decreased when the substrate concentration increased (Fig. 3). This behavior indicates that the production of formate from hydrogen carbonate may have significant substrate or product inhibition. Low K_m could be related to high substrate inhibition. Too high formate concentration may also be harmful for the enzyme activity. Figs. 4 and 5 show that the enzyme concentration and reaction time affect the reduction of hydrogen carbonate, thus allowing the optimization of reaction conditions. However, the resolving of the inhibition at high substrate concentration requires attention to improve the biotransformation ability of the enzyme.

Sequence comparison and modeling of active site residues in FDHs

The modeling of CtFDH sequence on 2NAD PDB structure of PseFDH showed that the residues around the substrate are exactly the same in CtFDH and PseFDH. The key amino acid residues for binding to the substrate are similar in all examined FDHs (Fig. 6). The nearest residues in PseFDH, CtFDH and TsFDH (distance 5 Å) are Pro97, Phe98, Gly121, Ile122, Asn146, Arg284, His332 and Gly335 in 2NAD numbering. Only one difference is appearing in CbFDH and CmFDH at position 122. There is small hydrophobic valine instead of bulky hydrophobic isoleucine. Therefore, substrate position in wider space allows more contacts to the active site residues (Schirwitz *et al.*, 2007).

HCO_3^- in the active site

The catalytic mechanism for formate oxidation is hydride transfer from formic acid to NAD^+ (Lamzin *et al.*, 1994; Tishkov and Popov, 2004; Castillo *et al.*, 2008). In general, the hydride transfer

Table II. The kinetic constants for different FDHs

FDH	Formate			Sodium hydrogen carbonate			References
	k_{cat} (s^{-1})	K_B(mM)	k_{cat}/K_B (1/mM.s)	k_{cat} (s^{-1})	K_B(mM)	k_{cat}/K_B (1/mM.s)	
CbFDH	1.081 ± 0.109	8.55 ± 2.56	0.126	0.015 ± 0.005	31.28 ± 8.05	0.0004	Choe *et al.*, (2014)
TsFDH	1.769 ± 0.441	16.24 ± 5.39	0.109	0.318 ± 0.051	9.23 ± 3.98	0.034	Choe *et al.*, (2014)
CmFDH	1.31 ± 0.02	7.01 ± 0.37	0.187	0.008 ± 0.000	0.78 ± 0.15	0.010	This study
CtFDH	2.039 ± 0.46	3.30 ± 0.26	0.618	0.023 ± 0.000	0.32 ± 0.07	0.069	This study

Buffers when formate is substrate: 20 mM acetate pH 5 for CtFDH, 100 mM sodium phosphate buffer pH 7.0 for both TsFDH and CbFDH, 20 mM phosphate pH 8 for CmFDH. Buffers when hydrogen carbonate is substrate: 20 mM phosphate pH 7.5 for CmFDH, 100 mM sodium phosphate buffer pH 7.0 for both TsFDH and CbFDH, 20 mM phosphate pH 8 for CtFDH. The substrate affinity constant K_B and the Michaelis–Menten constant K_m are not fully comparable.

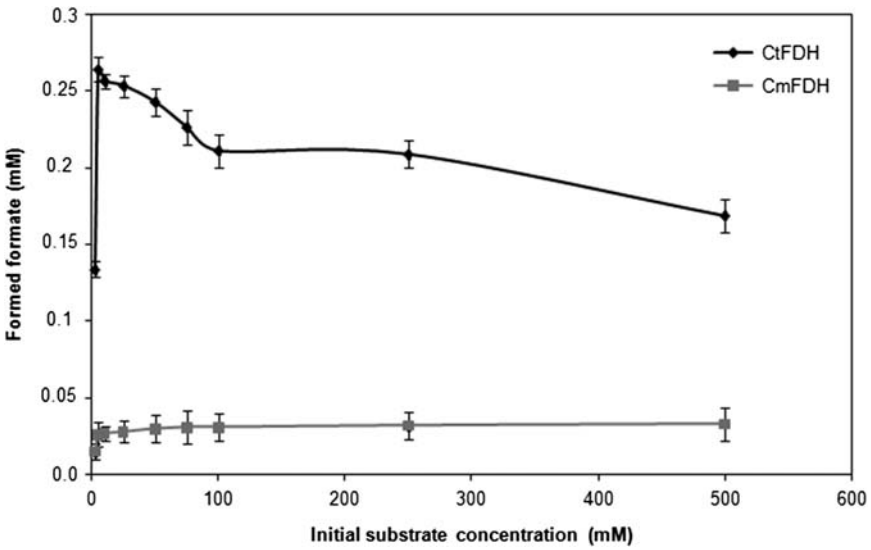


Fig. 3 Effect of initial substrate concentration on the activities of CmFDH and CtFDH for the reduction of hydrogen carbonate to formate.

Downloaded from https://academic.oup.com/peds/article-abstract/30/1/47/2585061 by Cukurova University Library (CU) user on 09 June 2020

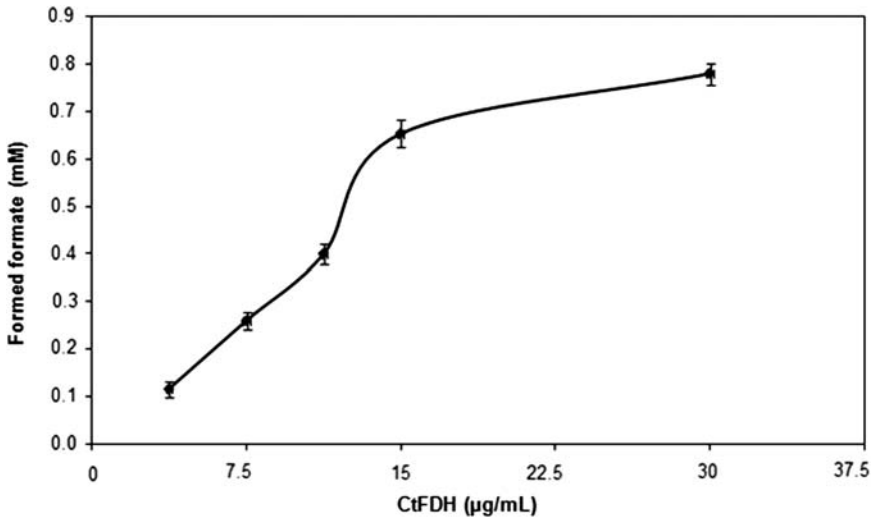


Fig. 4 Effect of CtFDH concentration on the reduction of hydrogen carbonate to formate.

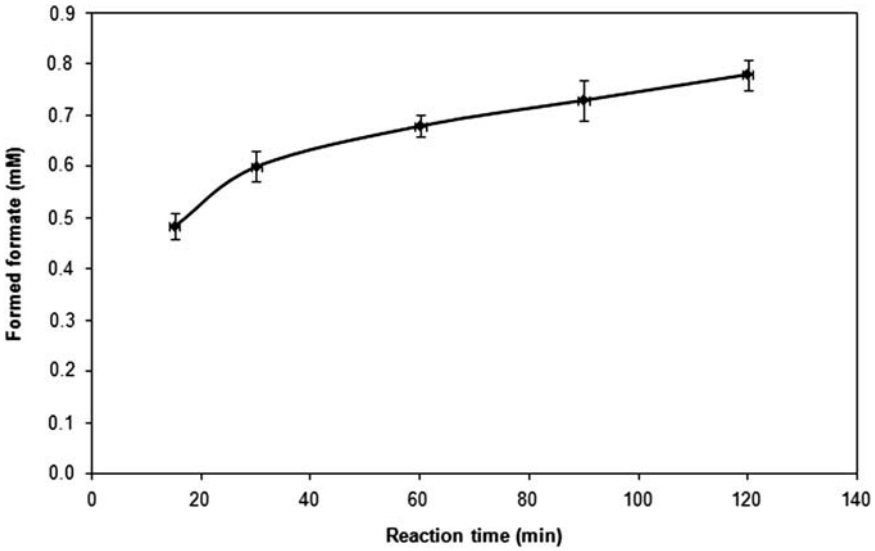


Fig. 5 Effect of reaction time on the reduction of hydrogen carbonate to formate by CtFDH.

path between substrate and coenzyme depends on the ratio of NAD^+ to NADH, which is the measure of the existing redox state. While the nicotinamide ring of NADH has a saturated carbon atom at Position 4, the aromatic *p* orbital system does not exist in the same form as in the NAD^+ (Kyte, 1995). During the oxidation ($NADH \rightarrow NAD^+$), the hydride is 'pushed off' from the saturated carbon C4 of NADH to the hydrogen carbonate. The conversion of NADH to NAD^+ is possible due to the rearrangement of the *p* orbital system in the nicotinamide ring, Schema 1. The reaction proceeds to the intermediate state, where the carbon-hydride bond is present with concomitant two negative oxygens. This kind of structure is very unstable (because of the repulsion of charges), and thus, the negative charges will push away the leaving hydroxyl group, resulting in the formation of a formate anion. In the active site interior, the hydride transfer can occur between the sp^3 hybridized hydrogen of C4 position and the sp^2 hybridized form of HCO_3 (carbonyl group) in dry environment, see Fig. 7.

It is possible that the carboxamide group of NADH exists in different orientations, since it is free to rotate, and the concurrent interactions of substrate can modify its position. Therefore, in Fig. 6, NADH is shown in two conformations, one is equal to that in the PDB structure 2NAD and the other is alternative. His332 is contacting to O3 of HCO_3^- with a hydrogen bond and O1 has hydrogen bonds to the amide proton at the backbone of Ile122 and the side chain ($-NH_2$) of Asn146. These contacts on both sides of HCO_3^- may help to keep it in place until the hydride ion from NADH attacks the carbon atom. The proximity of the positively charged Arg284 may assist the released hydroxide ion to exit the active site and enter the substrate channel. According to model 1 of the active site, the leaving –OH could move towards Arg284. The Arg284 residue is very important because of its conserved feature of acting as a vehicle (Nilov *et al.*, 2011). The alternative way is the protonation. In the active site, one of negatively charged oxygen of hydrogen carbonate could be protonated by the side chain of Asn146 or by the backbone amide of Ile122. The protonation by His332 can happen also to HCO_3 if at the same time the hydrogen bonding of Ile122 (between –OH and –C=O) takes place. The formate formation by hydride ion transferring from NADH to HCO_3

Downloaded from https://academic.oup.com/peds/article-abstract/30/1/47/2585061 by Cukurova University Library (CU) user on 09 June 2020

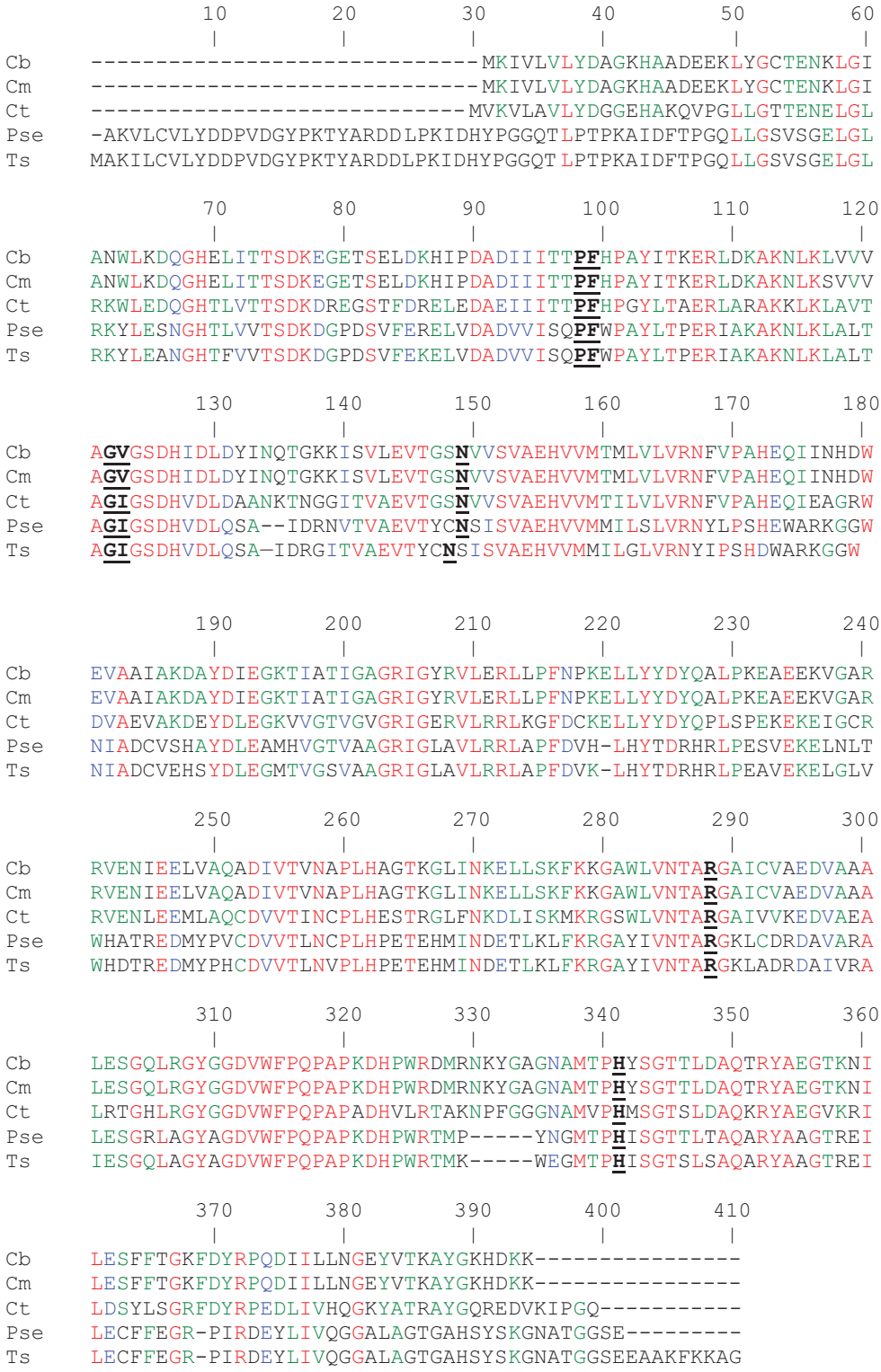
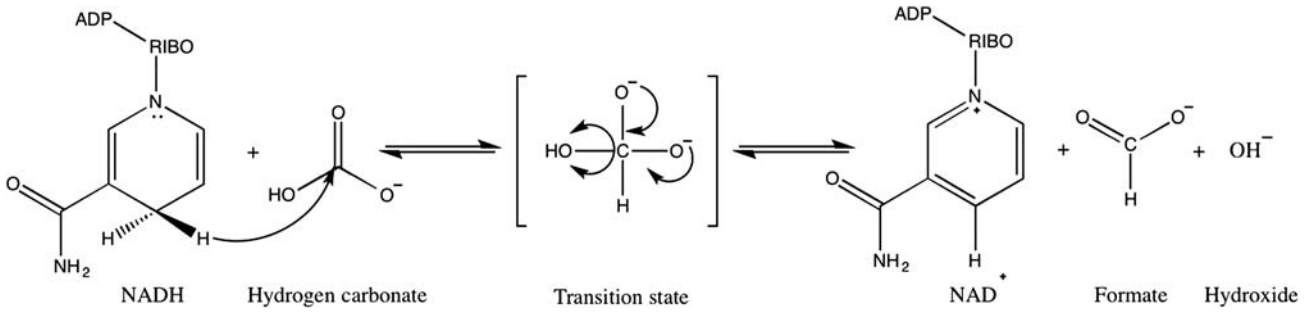


Fig. 6 Alignment of formate dehydrogenases. Symbols: Ps, *Pseudomonas* sp. (strain 101) (PseFDH); Cb, *Candida boidinii* (CbFDH); Ts, *Thiobacillus* sp. (strain KNK65MA) (TsFDH); Cm, *Candida methylica* (CmFDH); Ct, *Chaetomium thermophilum* (CtFDH). The nearest amino acid residues (distance 5 Å) to substrate in FDHs are shown by black bold and underline. The alignment was created by Multalin (https://npsa-prabi.ibcp.fr/cgi-bin/npsa_automat.pl?page=npsa_multalin.html).

Downloaded from https://academic.oup.com/peds/article-abstract/30/1/47/2585061 by Cukurova University Library (CU) user on 09 June 2020



Schema 1. Hydrogen transfers from NADH to hydrogen carbonate as hydride (H–).

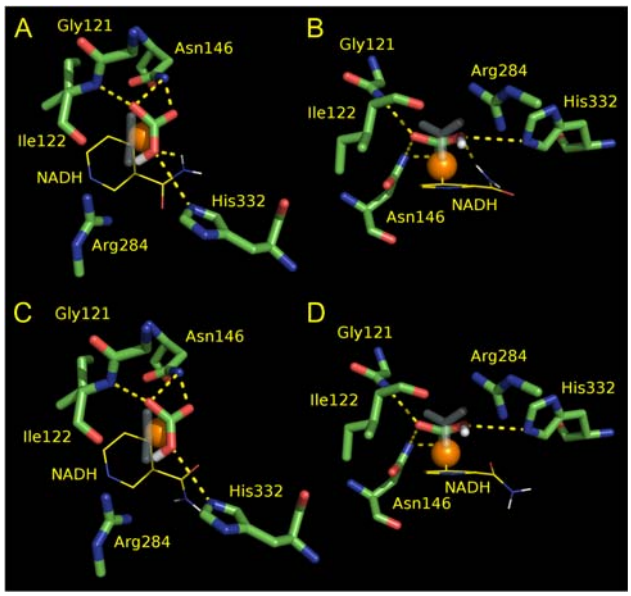


Fig. 7 Proposed models of hydrogen carbonate binding to the active site of CtFDH. In upper panel (**A**) on the left, the hydride bonded to the C4 of NADH (truncated, narrow lines) is shown as an orange sphere and the transparent white molecule indicates the position of formate as a reference. Orientation of the carboxamide group is shown as flipped 180°. Hydrogen bonds are represented by yellow dotted lines. On the right (**B**), the active site is viewed from another direction, emphasizing the differences between formate and hydrogen carbonate binding. In order for the hydride transfer to occur, the *p* orbital of the carbon atom of bicarbonate must be perpendicular to the hydride at C4 of NADH. In lower panel (**C** and **D**), the active site and substrates have same orientation as upper panel, but the carboxamide group of NADH is shown as in the PDB structure 2NAD for PseFDH (Lamzin *et al.*, 1994). The residue numbering is also according to 2NAD.

is not conclusively occurring in a step-by-step manner. Therefore, this reaction needs to be evaluated using molecular calculations and further simulation studies.

Conclusion

The enzyme activity assays showed that CtFDH is one of the most efficient known FDH enzymes in converting hydrogen carbonate to formate. The apparent decreasing of the reaction rate in high substrate concentration with hydrogen carbonate requires further development of the process design of even enzyme engineering to build more efficient catalytic systems for CO_2 fixation by FDH. The modeling indicated that hydrogen carbonate fits into the active site of PseFDH and CtFDH and revealed the apparent reaction steps from hydrogen carbonate to formate. In aqueous solution, HCO_3^- converts first to electrophile carbon dioxide, which then acts forwards as reactive substrate. We proposed that the active site of FDH may provide an alternative way in dry environment for reduction from hydrogen carbonate to formate. The analysis of the catalytic reaction in both directions indicates that the orientation of the hydrogen in the nicotinamide ring is different for the hydride leaving from NADH than for the hydride coming to NAD^+. When the hydride leaves from NADH, the angle is about 33° to the plane and the direction for the coming hydride is perpendicular. Therefore, hydrogen carbonate and formate in the active site have no identical positions during the catalysis. The modeling results could be utilized in designing more efficient mutant enzymes for CO_2 conversion to hydrocarbons.

Supplementary data

Supplementary data are available at *PEDS* online.

Funding

This work was supported by a grant from the TUBITAK (Grant number: 214Z292).

References

Alissandratos,A., Kim,H.K. and Easton,C.J. (2013) *Bioengineered*, **4**, 348–350.

Atsumi,S., Higashide,W. and Liao,J.C. (2009) *Nat. Biotechnol.*, **27**, 1177–1180.

Bassegoda,A., Madden,C., Wakerley,D.W., Reisner,E. and Hirst,J. (2014) *J. Am. Chem. Soc.*, **136**, 15473–15476.

Baxter,J., Bian,Z., Chen,G. *et al.* (2009) *Energy Environ. Sci.*, **2**, 559–588.

Binay,B., Alagöz,D., Yildirim,D., Çelik,A. and Tükel,S.S. (2016) *Beilstein Journal of Organic Chemistry*, **12**, 271–277.

Bonke,S.A., Wiechen,M., MacFarlane,D.R. and Spiccia,L. (2015) *Energy Environ. Sci.*, **8**, 2791–2796.

Castillo,R., Oliva,M., Martı,S. and V. Moliner,V. (2008) *J. Phys. Chem. B.*, **112**, 10012–10022.

Choe,H., Joo,J.C., Cho,D.H., Kim,M.H., Lee,S.H., Jung,K.D. and Kim,Y.H. (2014) *Plos One*, **9**, e103111.

Hartmann,T. and Leimkühler,S. (2013) *FEBS J.*, **280**, 6083–6096.

Kim,S., Kim,M.K., Lee,S.H., Yoon,S. and Jung,K.-D. (2014) *J. Mol. Catal. B: Enzym.*, **102**, 9–15.

Downloaded from https://academic.oup.com/peds/article-abstract/30/1/47/2585061 by Cukurova University Library (CU) user on 09 June 2020

Kuwabata,S., Tsuda,R. and Yoneyama,H. (1994) *J.Am.Chem.Soc.*, **116**, 5437–5443.

Kyte,J. (1995) Mechanisms in Protein Chemistry. Garland Publishing Inc, pp. pp. 27–30. Garland Publishing, Inc., New York & London.

Lamzin,V.S., Dauter,Z., Popov,V.O., Harutyunyan,E.H. and Wilson,K.S. (1994) *J.Mol. Biol.*, **236**, 759–785.

Lu,Y., Jiang,Z.-Y., Xu,S.-W. and Wu,H. (2006) *Catal. Today*, **115**, 263–268.

Mallick,N., Bagchi,S.K., Koley,S. and Singh,A.K. (2016) *Front Microbiol.*, **7**, 1019.

Moret,S., Dyson,P.J. and Laurenczy,G. (2014) *Nat. Communic.*, **5**, 4017.

Nilov,D.K., Shabalin,I.G., Popov,V.O. and Švedas,V.K. (2011) *Biochemistry (Moscow)*, **76**, 172–174.

Özgün,G., Karagüler,N.G., Turunen,O., Turner,N.J. and Binay,B. (2015) *J. Mol. Cat. B: Enzym.*, **122**, 212–217.

Schirwitz,K., Schmidt,A. and Lamzin,V.S. (2007) *Protein Sci.*, **6**, 1146–1156.

Shi,J., Jiang,Y., Jiang,Z., Wang,X., Wang,X., Zhang,S., Han,P. and Yang,C. (2015) *Chem. Soc. Rev.*, **44**, 5981–6000.

Tishkov,V.I. and Popov,V.O. (2004) *Biochemistry (Moscow)*, **69**, 1252–1267.

Wu,J.T., Wu,L.H. and Knight,J.A. (1986) *Clin. Chem.*, **32**, 314–319.

Downloaded from https://academic.oup.com/peds/article-abstract/30/1/47/2585061 by Cukurova University Library (CU) user on 09 June 2020